10th IMEKO TC14 Symposium on
Laser Metrology for Precision Measurement and Inspection in Industry
Braunschweig, GERMANY, 2011, September 12-14

Comparison of a Scanning Interferometric Profile Measurement Method and an Ultra-Precise Coordinate Measuring Machine

A. Wiegmann, **M. Schulz**, Physikalisch-Technische Bundesanstalt, Braunschweig;
K. Yoshizumi, Panasonic Corporation, Advanced Production Systems Development Company, Kadoma City Osaka,Japan;
K. Kubo, Panasonic Production Technology Co., Ltd, UA3P Development Team, Kadoma City Osaka, Japan;
D. Ramm, Panasonic Factory Solutions Europe a division of Panasonic Industrial Europe GmbH, Hamburg

Abstract:

Comparative profile measurements of a test specimen with a diameter of 150 mm and a peak-to-valley height of 50 µm carried out by an ultra-precise coordinate measuring machine (Panasonic UA3P) and a highly accurate scanning interferometric multi-sensor instrument (ETMS) are presented. The instruments and their principles are described. Although the measurement principles of the instruments are different, the measurements agree within the claimed uncertainties. The rms-difference of the measurement results is less than 20 nm.

Introduction

Interferometric topography measurements of nearly plane surfaces are possible with uncertainties at the nanometer or even sub-nanometer level. As interferometers are only comparative instruments, their reference surface has to be calibrated, e.g. by the three flat test [1] or by comparison to reference free deflectometric methods [2]. For non-flat surfaces, null lenses or computer generated holograms (CGH) [3] are used to allow for near normal incidence on the test surface. However, calibration of the null lens or the CGH is more difficult. An approach to make non-flat surfaces measurable by interferometry is sub-aperture stitching [4]. The drawback of this method is the accumulation of calibration errors of the reference surface. If the aperture of the interferometer is much smaller than the size of the specimen, even small calibration errors can accumulate to a large parabolic topography error. This accumulation can be avoided by using an additional angle measuring device as flatness reference [5,6]. The latest development of this technique was named the Extended

Traceable Multi Sensor (ETMS) technique. This technique aims at profile measurements of rather long specimens (up to one meter) with peak-to-valley (PV) heights up to 100 µm with measurement uncertainties in the nanometer range.

Another solution to measure non-flat surfaces are coordinate measuring machines (CMM). In the last few years, several highly accurate CMMs have been developed [7-9]. Focusing on the demands of the optical industry, at Panasonic an Ultrahigh Accurate 3-D Profilometer, called UA3P, was developed to meet these needs [10-12]. This profilometer can be applied to the form measurement of various optical surfaces. The position reference is realized by three calibrated plane mirrors arranged corresponding to the axis of a Cartesian coordinate system. The measurement uncertainty can be as low as 50 nm.

The ETMS principle and the measurement principle of the UA3P are basically different. This makes a comparison highly interesting. The principles of the two instruments and a comparison for a test surface are described in the following.

The test specimen

For the test specimen, a surface with a large PV height is reasonable, but it must still be measurable by the sub-aperture interferometer at each position. This restricts the maximum slope of the specimen. A measured profile of the utilized surface is shown in Fig. 1.

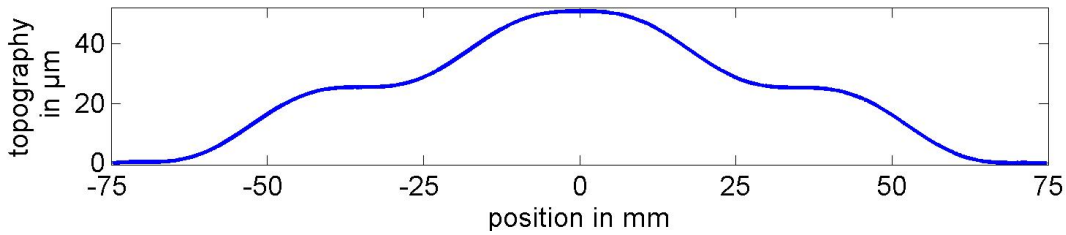

Fig. 1: Profile of the rotationally symmetric test specimen. The profile shown is the average of 20 ETMS measurements.

The diamond turned brass specimen has a diameter of 150 mm and a PV height of 50 µm. Due to the manufacturing process, the specimen may contain some contaminations with lateral dimensions smaller than the lateral resolution of the interferometer used for ETMS.

The ETMS system

The ETMS technique reconstructs the profile of the specimen from many sub-profiles. A compact phase shifting interferometer (aperture 3 mm, 165x165 pixels, pixel distance 19 µm) is moved over the specimen measuring small sub-profiles. Due to an imperfect calibration of the interferometer reference, each distance sensor (respectively pixel) j has an unknown

systematic error ε_j. In each measurement position i, the scanning stage introduces an offset a_i and a tilt b_i. The tilt b_i is measured in each position by an autocollimator. The position p_i of the sensor head is measured with a displacement interferometer (cf. Fig. 2).

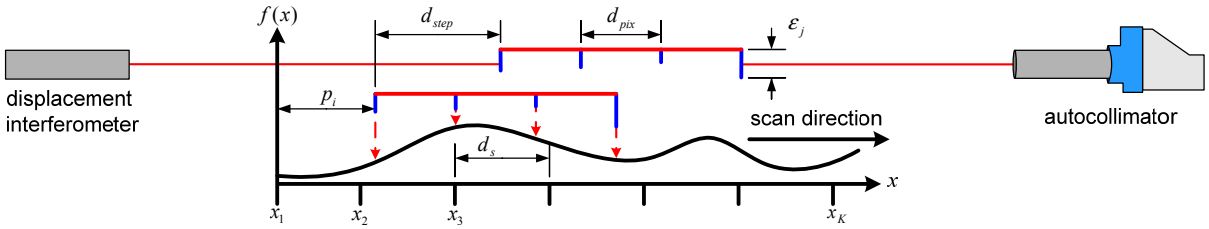

Fig. 2: Sketch of the Extended TMS method.

The measurement of the distance sensors j in the position i can be modeled as follows.

$$m_{i,j} = -\sum_{k=\left\lfloor \frac{\tilde{x}_{i,j}}{d_s} \right\rfloor - \frac{o-1}{2}}^{\left\lfloor \frac{\tilde{x}_{i,j}}{d_s} \right\rfloor + \frac{o-1}{2}} c_k(\tilde{x}_{i,j}) f(x_k) + \varepsilon_j + a_i + b_i s(j) \qquad \text{with} \qquad c_k(\tilde{x}_{i,j}) = \prod_{\substack{h=\left\lfloor \frac{\tilde{x}_{i,j}}{d_s} \right\rfloor - \frac{o-1}{2} \\ h \neq k}}^{\left\lfloor \frac{\tilde{x}_{i,j}}{d_s} \right\rfloor + \frac{o-1}{2}} \frac{\tilde{x}_{i,j} - x_h}{x_k - x_h} \qquad (1)$$

The topography f is modeled at the positions x_k. By the application of Lagrange interpolation, a continuous topography model is introduced allowing for measurement positions $\tilde{x}_{i,j}$ in-between the x_k. The index o is the degree of the interpolation polynomial. For the measurements of the test specimen, o was set to 41. Note that (1) is linear in the unknowns $f(x_k)$, ε_j, a_i and b_i provided that the sensor positions s(j) are known. A system of linear equations can be constructed to estimate these unknowns. As shown in [5], a unique reconstruction (up to an unknown straight line) of the topography values $f(x_k)$ is only possible if the b_i are measured in addition and added to the system of linear equations. Apart from estimates of the topography values $f(x_k)$, the solution of the system of linear equations delivers also estimates of the offsets a_i, the tilts b_i and the systematic errors ε_j.

The ETMS technique allows the reconstruction distance d_s to be smaller than the scanning step d_{step} if non-equidistant scanning steps are used. The interferometer was therefore moved over the specimen with scanning steps between 0.6 mm and 1 mm resulting in overall 186 measurement positions allowing for d_s=20 µm (7468 topography points).

The average of 20 ETMS measurements was already shown in Fig. 1. The standard uncertainty of one profile measurement with the described measurement setup has been evaluated with Monte Carlo simulations according to [13] and is shown in Fig. 3. The main

uncertainty source for an ETMS measurement is the effective pixel distance of the

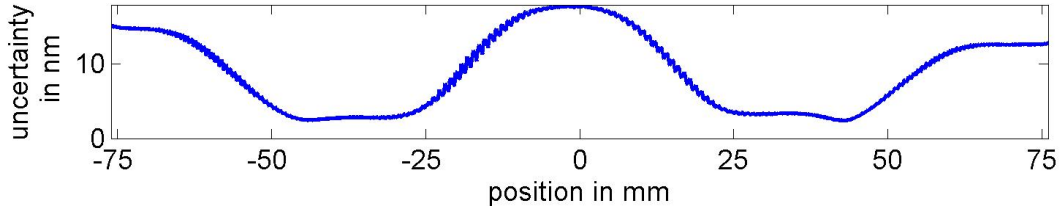

Fig. 3: Standard uncertainty for one profile measurement with the described ETMS setup. The average uncertainty is 9 nm and the maximum uncertainty 18 nm.

interferometer. If the value of the effective pixel distance which is used for the reconstruction is too small, the PV height of the reconstructed topography is too large and vice versa. This is the reason for the characteristic form of the uncertainty graph in Fig. 3. Therefore, the effective pixel distance is calibrated before every measurement. The calibration of the effective pixel distance d_{pix} can be undertaken with an uncertainty of about 15 nm.

The UA3P coordinate measuring machine

The Panasonic UA3P Ultrahigh Accurate 3-D Profilometer using a high accuracy three axes laser interferometer was developed in 1987 [10] and the Atomic Force Probe (AFP) was developed in 1993 [11]. The UA3P using AFP was launched on the market in 1994.

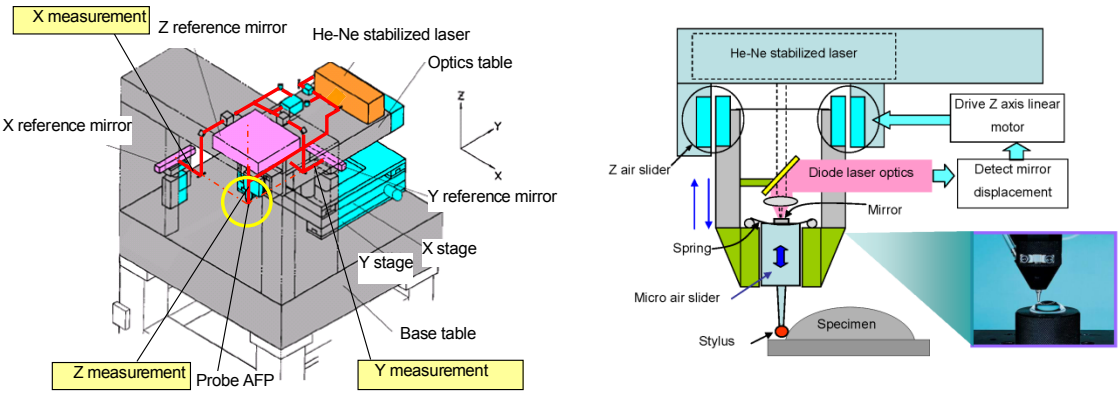

Fig. 4: Three axes laser interferometer of the UA3P (left) and the Atomic Force Probe (AFP) and Z axis servo control (right).

Aspheric lenses that could not be made with high quality before the development of the UA3P, because they could not be measured, have since been developed and mass produced. Many new products using aspheric lenses such as DVD players, digital cameras, mobile phones, laser printers and optical communications are widely spread. UA3Ps are used as measuring systems of highest accuracy by lens manufacturers. The UA3P high accuracy three axes laser interferometer is shown in Fig. 4 (left). A stabilized He-Ne laser is

used for the XYZ measurement. Its wavelength is highly stable and is traceable to the SI unit of length. The AFP can be moved in the XYZ directions along XYZ reference mirrors which are fixed to the base table. The XYZ coordinates are measured almost at the exact level of the AFP, so the straightness error does not cause a significant measurement error. The principle of the Atomic Force Probe is shown in Fig. 4 (right).

The measuring force is 0.15-0.30 mN. The measurement speed in XY directions is 0.01-20 mm/s, and is variable according to the models. The stylus tip radius is 500 µm when using a ruby sphere (as used for the test specimen) and 2 µm for a diamond stylus which can be used instead. The measurable slope angle is from 0° to 75°. The repeatability when measuring a plane mirror with a length of 25 mm five times was 2.3 nm (standard deviation) [12].

There are four types of UA3P. For the comparison, the UA3P-5 with a measurement range of 200 mm, 200 mm and 45 mm in X, Y, and Z was used. Though UA3P is a reliable standard machine, it can not measure a larger range, such as for example 1 m X-ray mirrors.

Comparison of the measurement results

With the ETMS setup only one profile of the specimen has been evaluated; with the UA3P, 41 separate profiles with a lateral displacement of 100 µm have been measured. The distance between neighbouring topography points of one UA3P measurement is 50 µm, and is 20 µm for the ETMS measurement. For the comparison of the measurement results, the ETMS measurement result has been rotated and shifted relative to each of the UA3P measurements till the rms-deviation is minimal. Figure 5 shows the achieved rms-differences

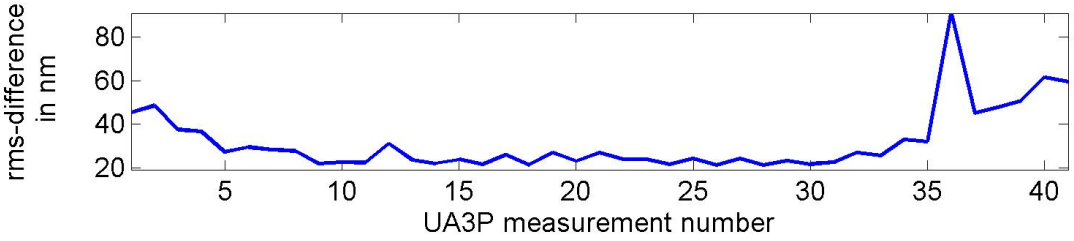

Fig. 5: Rms-difference between the ETMS measurement result and the UA3P measurements.

after the alignment procedure. The rms-difference for the inner 20 UA3P measurements is marginally larger than 20 nm. The rms-difference of the first 10 and the last 10 profiles measured by the UA3P is larger due to the change of the specimens profile. The minimal rms-difference is 21.1 nm (UA3P measurement number 26). The difference between both topographies is displayed in Fig. 6. Several peaks with heights up to 200 nm appear in the

difference topography. These peaks are responsible for a substantial part of the resulting rms-value. As can been seen in Fig. 6, these peaks are not caused by normal noise, since all

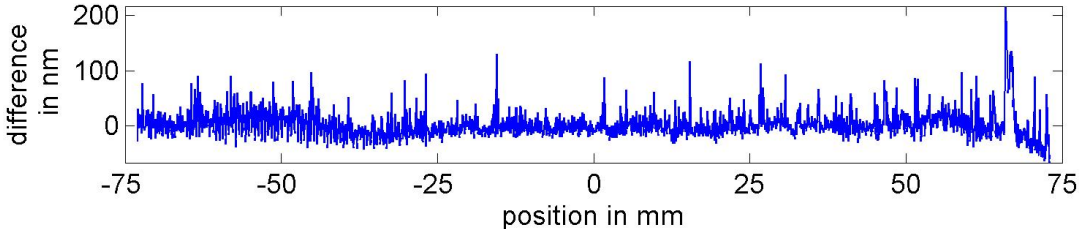

Fig. 6: Difference topography between the ETMS measurement and the UA3P measurement.

of them depart in the same direction. Most of the peaks are caused by the production process of the specimen which generates some small non-removable metal particles. The lateral dimension of these particles is smaller than the lateral resolution of the interferometer used for the ETMS measurements. Hence, these small particles are not visible in the ETMS measurements. The UA3P, in contrast, resolve these particles as small peaks with heights of some hundred nanometers. This is a basic difference between both measurement techniques. The ETMS technique aims at the form of the specimen given by wavelengths greater than $2d_s$ [14] while the UA3P aims at the local topography height at the measurement locations. For further comparison of the measurement results, peaks departing more than 70 nm from a best-fit polynomial of degree 30 have been removed from the UA3P measurements. From the total of 2877 measured points only 33 have been removed resulting in an rms-difference of only 18.1 nm.

The maximum measurement uncertainty of the ETMS profile measurement is 18 nm, the uncertainty of one UA3P profile measurement is 50 nm. In contrast to the ETMS measurement, the measurement uncertainty for the UA3P is the same for each point of the profile and independent of the profile of the specimen under test. Nevertheless, both measurements agree within their measurement uncertainties. The remaining differences in Fig. 6 may be caused by different holders of the specimen, or the not exact matching of the position of the profiles which have been compared. Apart from the above mentioned peaks, no systematic differences between the tactile and the optical measurement could be observed within the claimed measurement uncertainties.

Conclusion

Tactile and optical measurement results for a nearly flat specimen with a diameter of 150 mm and a PV height of 50 µm have been presented. Both measurement results agree within their

uncertainties, which are 18 nm for the optical (ETMS) and 50 nm for the tactile measurement (UA3P). A systematic difference between both measurement techniques is the response of the measurement devices to local features of the specimen under test. Whereas the tactile measurement technique is able to measure these local form deviations, the optical measurement reconstructs only that part of the specimen given by the lower spatial frequencies of the specimen. The measurements' results show an rms-difference of 21.1 nm or respectively 18.1 nm if the peaks of the tactile measurement are removed. Hence, care must be taken in the choice of the correct measurement technique. If the measurement aims at the long-wave form of the specimen the presented optical measurement technique is preferable. However, if the local height of the specimen at selected positions of the specimen is of interest, the tactile measurement technique should be preferred.

References

[1] U. Griesmann; *Appl. Opt.* 45 (2006), 5856–65.

[2] I. Weingärtner, M. Schulz, C. Elster; *Proc. SPIE* (1999), 3782 306–17.

[3] S. Reichelt, H. Tiziani; *Technisches Messen* 73 (2006), 554–65.

[4] M. Bray; *Proc. SPIE* (1999), 3739 259-273.

[5] C. Elster, I. Weingärtner, M. Schulz; *Prec. Eng.* 30 (2006), 32–8.

[6] A. Wiegmann, M. Schulz, C. Elster; *Optics Express* 16 (2008), 11975–86.

[7] IBS, ISARA Ultra Precision CMM http://www.ibspe.com/ibs_precision_engineering_du/pdfs/Isara.pdf [Online; accessed 02-May-2011].

[8] Zeiss F25Microsystem CMM http://www.zeiss.com/4125682000247242/Contents-Frame/5b1a8ebc2a5e14b886257154006ae1a3 [Online; accessed 02-May-2011].

[9] E. Jäger, E. Manske, T. Hausotte, H.-J Büchner; *Technisches Messen* 67 (2000), 319–23.

[10] K. Yoshizumi, T. Murao, J. Masui, R. Imanaka, Y. Okino; *Appl. Opt.* 26 (1987), 1647–53.

[11] K. Yoshizumi, K. Kubo; *National Technical Report* 39 (1993), 598–603.

[12] H. Takeuchi, K. Yosizumi, H. Tsutsumi; *ASPE Proceedings, Free-Form Optics* (2004).

[13] ISO 2008 *Guide to the expression of uncertainty in measurement (GUM)-Supplement 1: Propagation of distributions using a Monte-Carlo method*.

[14] A. Wiegmann, M. Schulz, C. Elster; *Optics Express* 17 (2009), 11098–106.